JOURNAL OF VIROLOGY, July 2006, p. 6411–6419 Vol. 80, No. 13
0022-538X/06/$08.00+0 doi:10.1128/JVI.00239-06

Intracellular Activated Notch1 Is Critical for Proliferation of Kaposi's Sarcoma-Associated Herpesvirus-Associated B-Lymphoma Cell Lines In Vitro

Ke Lan, Tathagata Choudhuri, Masanao Murakami, Daniel A. Kuppers, and Erle S. Robertson*

Department of Microbiology and Tumor Virology Program of Abramson Comprehensive Cancer Center, University of Pennsylvania Medical School, Philadelphia, Pennsylvania 19104

Received 2 February 2006/Accepted 29 March 2006

Kaposi's sarcoma-associated herpesvirus (KSHV) is a human tumor virus expressing latent antigens critical for pathogenesis. The mechanism by which KSHV mediates oncogenesis has not been fully elucidated. Notch signaling is an evolutionarily conserved pathway controlling diverse events related to development, proliferation, and tissue homeostasis. Deregulation of Notch signaling has also been shown to be highly correlated with oncogenesis. Here we show that the activated intracellular domain of Notch1 (ICN) is aberrantly accumulated in latently KSHV-infected pleural effusion lymphoma cells and results in increased proliferation. Specifically, growth of the infected cells was dramatically inhibited at the G_1 phase by treatment with a γ-secretase inhibitor which specifically blocks the production of ICN. Increased ICN also up-regulated the cyclin D1 cell cycle regulator. Taken together, these studies define an important mechanism directly linking latent KSHV infection to induction of oncogenesis through dysregulation of the conserved Notch signaling pathway.

Kaposi's sarcoma-associated herpesvirus (KSHV) is a gamma-2 herpesvirus and is the infectious agent important for the development of Kaposi's sarcoma (KS) as well as specific lymphoproliferative disorders in humans (9, 14). Globally, these cancers are some of the most common cancers with an etiological link (8). Ninety genes are carried by the KSHV genome (48), but <10% of these genes are expressed during latency, which is quickly established after primary infection (44). KSHV-associated KS and pleural effusion lymphomas (PELs) express these latent genes, which are capable of dysregulating cell cycle apoptotic pathways as well as providing evasion strategies from host immune responses (19).

Following primary lytic infection, KSHV typically establishes a latent form of infection (33, 42, 43). However, there are always small percentages of cells automatically undergoing lytic replication. To date, it is well accepted that both latency and lytic reactivation contribute to viral pathogenesis (19). The diversity of the KSHV genes allows the virus to interact with and modulate the cellular activities of its host cell by utilizing a number of different strategies. These effects can promote a number of specific changes in the infected cells, leading to pathogenesis. The latency-associated nuclear antigen (LANA) is a multifunctional protein and is predominantly expressed during viral latency. Besides maintenance of the episomal DNA (4, 5, 17), LANA has also been shown to interact with cellular molecules and to down-regulate their activity. LANA also interacts with the tumor suppressors p53 and pRb, leading to the blockage of apoptosis and cell cycle deregulation mediated by these tumor suppressors (21, 39). Additionally, LANA has also been shown to regulate various other cellular pathways, including the Wnt signaling pathway, by stabilizing beta-catenin by binding to the negative regulator glycogen synthase kinase 3β, causing a cell cycle-dependent nuclear accumulation of glycogen synthase kinase 3β (22, 23). LANA was also shown to transactivate the telomerase reverse transcriptase promoter, which has also been shown to contribute to the oncogenic phenotype (30). In the natural host, KSHV is usually seen as a coinfection with human immunodeficiency virus and/or Epstein-Barr virus (EBV) (11, 13, 38). LANA has also been shown to modulate the transcriptional activity of the human immunodeficiency virus long terminal repeat promoter and to transactivate the LMP1 and Cp promoters of EBV, which may also contribute to oncogenesis (27, 28, 41). Most recently, our laboratory has demonstrated that LANA causes chromosome instability in KSHV-infected B cells (47). These studies suggest that LANA contributes to driving oncogenesis in KSHV-infected cells. However, the mechanisms involved in this process have only partially been understood. Therefore, further studies are necessary to provide a more comprehensive picture of the role of LANA in KSHV-mediated oncogenesis.

Notch signaling is an evolutionarily conserved pathway controlling diverse aspects of development and tissue homeostasis (1, 26). Deregulation of Notch signaling has been implicated in the development of cancer, with the intracellular form of Notch1 (ICN) being associated with a subset of human T-cell lymphomas and with tumorigenesis in animal model systems (20, 25, 29). In this report, we show that ICN is accumulated in KSHV-positive cells and that this accumulation is mediated by KSHV LANA, resulting in an increased proliferation rate of the cells. ICN also plays an essential role in KSHV's ability to prolong the life-span of KSHV-infected human primary B cells. We also found that cyclin D1 expression is elevated, which can lead to increased cell cycle progression, and that this elevation of cyclin D1 is a downstream event of ICN in the

* Corresponding author. Mailing address: Department of Microbiology and Tumor Virology Program of Abramson Comprehensive Cancer Center, University of Pennsylvania Medical School, 201E Johnson Pavilion, 3610 Hamilton Walk, Philadelphia, PA 19104. Phone: (215) 746-0114. Fax: (215) 898-9557. E-mail: erle@mail.med.upenn.edu.

context of KSHV-infected B cells. These findings establish a link between KSHV-driven oncogenesis and Notch1, an important signaling molecule in numerous cellular processes, and demonstrate a unique mechanism by which KSHV can usurp this signaling pathway to drive the oncogenic process. In addition, a γ-secretase inhibitor (6) slows down the proliferation of KSHV-positive cells and induces the death of human primary B cells infected with KSHV. This suggests that pharmacologic manipulation of the Notch signaling pathway may have therapeutic potential in treating KSHV-positive cancers.

MATERIALS AND METHODS

Antibodies, cell lines, inhibitors, and plasmids. A KSHV Rta rabbit polyclonal antibody was provided by Gary S. Hayward (Johns Hopkins University School of Medicine). A KSHV Rta mouse monoclonal antibody was a kind gift from Koichi Yamanishi (Osaka University, Osaka, Japan). A human polyclonal serum which recognizes LANA is designated HS and was provided by Gary Nabel (Vaccine Institute, NIH, Bethesda, MD). Anti-Notch rabbit antiserum was provided by Jon C. Aster and Elliott Kieff (Brigham and Women's Hospital, Boston, MA). The Val1744 antibody was purchased from Cell Signaling Technology Inc., Beverly, MA.

Human embryonic kidney fibroblast 293 cells were obtained from Jon Aster (Brigham and Women's Hospital, Boston, MA). Ramos, Loukes, and DG75 are KSHV-negative B-cell lines isolated from Burkitt's lymphomas and were provided by Elliott Kieff (Harvard Medical School, Boston, MA). BCBL1 and BC3 are KSHV-positive, body-cavity-based lymphoma-derived cell lines and were obtained from Don Ganem (University of California School of Medicine, San Francisco, CA) and the American Type Culture Collection, respectively. JSC1 was a kind gift from Richard F. Ambinder (Johns Hopkins University School of Medicine, Baltimore, MD). Vero cells stably infected with Bac36 (Vero/Bac36) were provided by Shoujiang Gao (The University of Texas Health Science Center, San Antonio, TX). A human osteosarcoma cell line, U2OS, was obtained from the American Type Culture Collection.

Human embryonic kidney fibroblast 293 and 293T cells were grown in high-glucose Dulbecco's modified Eagle's medium supplemented with 5% bovine growth serum (BGS; HyClone Inc., Logan, UT), 2 mM L-glutamine, 25 U/ml penicillin, and 25 μg/ml streptomycin. Ramos, Loukes, DG75, BCBL1, BC3, and JSC1 cells were grown in RPMI 1640 medium supplemented with 10% BGS, 2 mM L-glutamine, 25 U/ml penicillin, and 25 μg/ml streptomycin.

A γ-secretase inhibitor {*N*-[*N*-(3,5-difluorophenacetyl-L-alanyl)]-*S*-phenylglycine *t*-butyl ester} was purchased from Calbiochem Inc. (San Diego, CA).

Hemagglutinin-tagged Notch ICN, pflu-ICN, and untagged pCDNA3.1-ICN expression vector were described previously (3). Myc-tagged LANA (pA3M-LANA) was described previously (31–33). The cyclin D1 reporter plasmid was a kind gift from Nancy Raab-Traub (University of North Carolina, Chapel Hill, NC).

Transfection. DG75 or BCBL1 cells were transfected by electroporation, using a Bio-Rad Gene Pulser II electroporator. Ten million cells harvested in exponential phase were collected and washed in phosphate-buffered saline (PBS) and then resuspended in 400 μl of RPMI or Dulbecco's modified Eagle's medium with DNA for transfection. Resuspended cells were transferred to a 0.4-cm cuvette and electroporated at 975 μF and 220 or 250 V. The electroporated cells were then transferred to 10 ml of complete medium, followed by incubation at 37°C and 5% CO_2. Transfected cells were harvested after 24 h and assayed for activity.

Induction of KSHV lytic replication and infection. To prepare KSHV-green fluorescent protein (KSHV-GFP) recombinant virus particles, we collected approximately 500 million exponentially growing Vero/Bac36 cells for induction. The procedures for preparation of infectious virions and for infection of cells were described previously (33).

Real-time reverse transcription-PCR. Real-time quantitative PCR was used to make a relative quantitative comparison of Notch levels in different cell lines. The procedure and method for calculation were described previously (33). The primers in this experiment were for Notch (5′ GGGCTTCAAAGTGTCTGAGG 3′ and 5′ CGGAACTTCTTGGTCTCCAG 3′) and β-actin (5′ GCTCGTCGTCGA CAACGGCTC 3′ and 5′ CAAACATGATCTGGGTCATCTTCTC 3′).

Immunofluorescence. Immunofluorescence assays were performed essentially as described previously (31–33). Slides were visualized with an Olympus XI70 inverted fluorescence microscope (Olympus Inc., Melville, NY) and photographed using a digital PixelFly camera and software (Cooke Inc., Warren, MI).

Flow cytometry. All flow cytometric analyses were conducted on a FACSCalibur cytometer (Becton Dickinson Inc., San Jose, CA), and analysis was done with FlowJo software (Tree Star, Ashland, OR). In carboxyfluorescein diacetate succinimidyl ester (CFSE) labeling experiments, briefly, 5 million cells were washed and incubated with 2.5 μM CFSE (Molecular Probes, Inc., Eugene, OR) in PBS for 10 min in the dark at room temperature. Unbound CFSE was quenched by the addition of BGS. The labeled cells were washed twice with 5% BGS in PBS and replated at a concentration of 300,000 cells per ml in RPMI 1640 medium containing 10% BGS. After 48 h in culture, cells were collected, fixed, and subjected to fluorescence-activated cell sorting (FACS) analysis. In cell viability analysis experiments, cells were collected, washed, and incubated with 10 μl 7-aminoactinomycin D (7AAD) (Pharmingen, San Jose, CA) for 10 min in the dark at 4°C. Five hundred microliters of PBS was then added, and cells were taken for FACS analysis immediately. $7AAD^+$ cells are referred to as dead cells.

For determination of the cell cycle phase distribution of nuclear DNA, untreated or gamma secretase inhibitor (GSI)-treated DG75 and BCBL1 cells (1×10^6 cells in each case) were harvested. Cells were fixed with chilled methanol and permeabilized with 0.5% Triton X-100, and nuclear DNA was labeled with propidium iodide (PI; 125 mg/ml) after RNase treatment. The cell cycle phase distribution of nuclear DNA was determined on a FACSCalibur instrument using Cell Quest software (Becton Dickinson, Franklin Lakes, NJ) and a fluorescence (FL2-A) detector equipped with a 488-nm argon laser light source and a 623-nm band-pass filter (linear scale). A total of 10,000 events were acquired for analysis. A histogram display of DNA content (*x* axis [PI fluorescence]) versus cell count (*y* axis) was created. CellQuest statistics were employed to quantitate the data at different phases of the cell cycle.

Luciferase assay. U2OS cells were collected at 70% confluence. One million cells were collected for transfection by using Lipofectamine 2000. The cells were subsequently lysed with 200 μl reporter lysis buffer (Promega, Inc., Madison, WI). Forty microliters of the lysate was mixed with 100 μl of luciferase assay reagent. Luminescence was measured for 10 s by an Opticomp I luminometer (MGM Instruments, Inc., Hamden, CT). The lysates were also tested at various dilutions to ensure that luciferase activities were within the linear range of the assay. The results shown represent experiments performed in triplicate.

RESULTS

Expression of Notch ICN is up-regulated in KSHV-positive cells. Previously, we and others showed that KSHV LANA and Rta can modulate viral gene expression though targeting recombination signal sequence-binding protein (RBP)-Jκ, the major downstream effector of the Notch1 signaling pathway (31, 33–35). Notch is a transmembrane receptor whose signaling is triggered by ligand binding (1, 26). Typically, protease-based cleavages lead to the production of ICN, which then translocates to the nucleus and binds to RBP-Jκ to modulate the expression of its downstream genes (51). Since we and others had shown that RBP-Jκ may be a critical control molecule for regulating the KSHV latency-to-lytic-infection switch (31, 34, 35), we wanted to explore the expression levels of ICN in KSHV-infected PEL cells, as ICN may also have an impact on KSHV in terms of regulation of the viral life cycle or on KSHV-mediated pathogenesis in the virus-host environment. To determine the expression of ICN in KSHV-infected PELs, Western blot analysis of the PEL cell lines BCBL1, BC3, and JSC1, which are all latently infected with KSHV, was performed. The results showed dramatically elevated levels of ICN in KSHV-positive PEL cells compared to those in the KSHV-negative B-lymphoma cell lines Ramos, Loukes, and DG75 based on signals from the ICN-specific antibody Val1744 (Fig. 1A). These findings were further corroborated by immunostaining of ICN in these cells. LANA was typically expressed in the nuclei of all KSHV-positive cells, with a characteristic punctate pattern which indicates the existence of the virus (Fig. 1B, upper panels), but there were no detectable levels of LANA in KSHV-negative cells (Fig. 1C, upper pan-

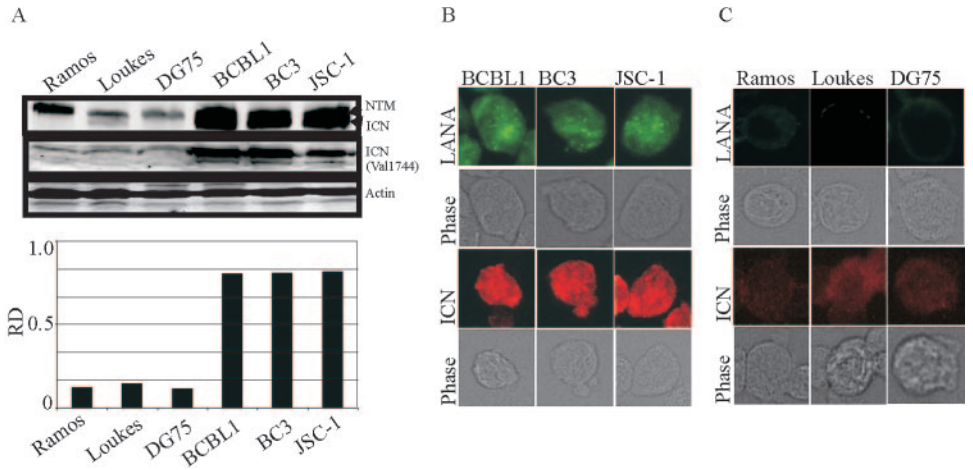

FIG. 1. Notch ICN is accumulated in KSHV-infected cells. (A) Western blot showing ICN levels in different cells. Cell lysates of Ramos, Loukes, DG75, BCBL1, BC3, and JSC1 cells were separated in an 8% sodium dodecyl sulfate-polyacrylamide gel, transferred to nitrocellulose membrane, and then blotted with anti-Notch rabbit serum. This antiserum recognizes the uncleaved transmembrane subunit NTM (upper band) and its intracellular cleavage product, ICN (bottom band). The same samples were also blotted with the Val1744 antibody, which specifically recognizes ICN. The loading amounts of lysates were normalized by the Bradford assay. Quantification of the relative density (RD) of ICN in each cell is also shown. (B and C) Cells were fixed and stained with anti-LANA human serum or the Val1744 rabbit polyclonal antibody, which specifically recognizes ICN. Staining was visualized with goat anti-human–fluorescein isothiocyanate or goat anti-rabbit–Texas Red antibodies.

els). Interestingly, ICN was strongly positive in KSHV-infected PEL cells (Fig. 1B, bottom panels) compared to the weak ICN signals in KSHV-negative B-cell lines (Fig. 1C, bottom panels).

Accumulation of Notch ICN is correlated with KSHV infection and LANA expression. The above data demonstrated that ICN is highly expressed in KSHV-positive cells compared to KSHV-negative cells of the same B-cell origin. However, these results did not determine if the accumulation of ICN in KSHV-positive cells was due to KSHV infection. To determine if KSHV infection mediates ICN accumulation, 293 cells were infected with Bac36, a recombinant KSHV expressing GFP which enables monitoring of viral infection (52). Bac36 has a similar gene expression profile to that of wild-type KSHV (52). By using Bac36, we can easily compare gene expression levels between KSHV-positive (infected) and -negative (uninfected) cells within the same isogenic background of the cell culture system. At 24 h postinfection, GFP signals were observed, followed by preparation of the cells for immunofluorence analysis. Immunostaining showed strong ICN signals in KSHV-infected, GFP-positive cells. As expected, low levels of ICN were observed in GFP-negative, uninfected cells (Fig. 2A). To further support these studies, we also harvested 293 cells infected with KSHV virions induced from BCBL1 at different time points to determine the levels of ICN. The results of Western blot analysis indicated that ICN began to accumulate at 24 h postinfection (Fig. 2B), the time at which KSHV typically establishes latency after infection and at which LANA's expression reaches a consistently high level.

LANA expression is critical for accumulation of ICN in human B cells. It has been shown that simian virus 40 (SV40) can up-regulate ICN through transcriptional regulation (7). To address the potential mechanisms for ICN accumulation in KSHV-infected cells, we employed real-time PCR to determine the transcription levels of Notch1 in different cell lines; however, the mRNA levels of Notch1 were similar in both KSHV-positive and -negative cells (data not shown). This indicates that ICN accumulation is likely mediated by a post-translational mechanism. Additionally, our data above demonstrated that ICN levels correlated with establishment of viral latency. Since LANA is predominantly expressed in latently KSHV-infected cells, we chose LANA as our target and hypothesized that LANA may be responsible for ICN accumula-

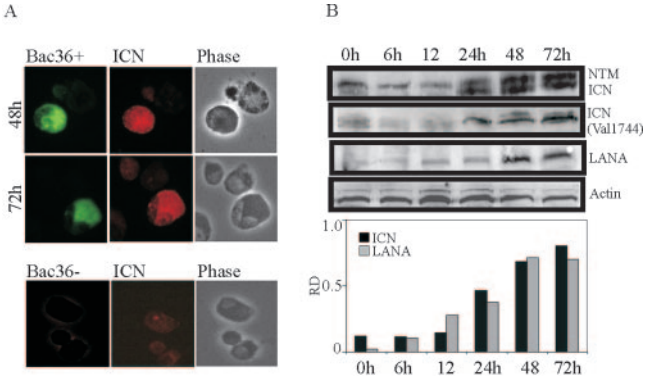

FIG. 2. (A) ICN is accumulated in de novo KSHV-infected cells. Twenty million Vero cells stably infected with the Bac36 KSHV-GFP recombinant virus were induced with tetradecanoyl phorbol acetate (20 ng/ml) and sodium butyrate (1.5 mM) for 4 days, and then the supernatant was filtered with a 0.45-μm filter and concentrated for each infection of 293 cells. At 48 h or 72 h postinfection, cells were fixed and stained with Val1744 antibody. Staining was visualized with goat anti-rabbit–Texas Red antibody. Virus existence was determined by the GFP marker. (B) ICN is up-regulated in KSHV-challenged cells. For each infection, 50 million BCBL1 cells were induced with tetradecanoyl phorbol acetate and sodium butyrate as described above. The supernatant was filtered with a 0.45-μm filter and concentrated by centrifugation at 18,000 rpm for 2 h; the virion pellet was resuspended in 100 μl PBS for inoculation of 293 cells. Cells were harvested at different times postinfection, and cell lysates were made for Western blot analysis. The relative densities (RD) of ICN and LANA in each cell treated with virus are also shown.

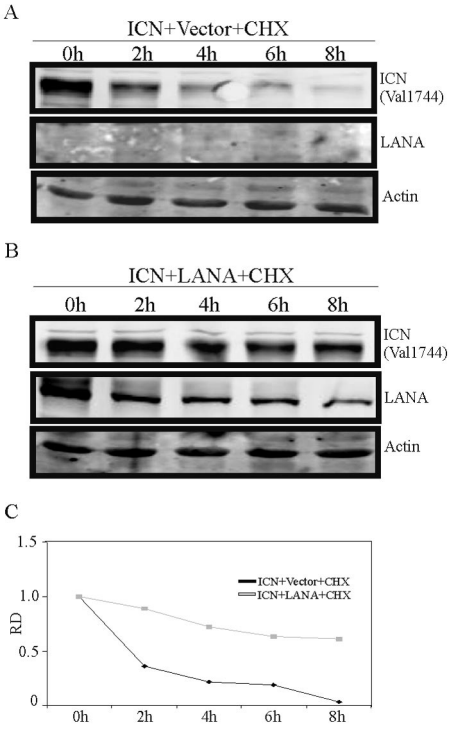

FIG. 3. LANA stabilizes ICN. For each transfection, 15 million DG75 cells were transfected with 10 μg ICN without (A) or with (B) 10 μg LANA. At 24 h posttransfection, cells were treated with cycloheximide at 100 μg/ml. At 0 h, 2 h, 4 h, 6 h, and 8 h posttreatment, cells were harvested for Western blot analysis. The relative density (RD) of ICN in each sample is also shown (C).

tion. DG75 cells were transfected with the ICN expression vector, with or without LANA, followed by cycloheximide treatment at 24 h posttransfection to inhibit new protein synthesis (36). By 2 h posttreatment, the ICN level was rapidly decreased in control cells and was barely detectable by 8 h (Fig. 3A). However, in the presence of LANA, ICN levels remained relatively constant for 8 h (Fig. 3B). These results strongly suggest that LANA can play a prominent role in regulating ICN stability and degradation.

Accumulation of Notch ICN results in increased cellular proliferation and plays a critical role in KSHV-mediated transformation. As we mentioned previously, aberrant Notch signaling is highly associated with oncogenesis. To determine the functional consequences associated with the accumulation of ICN in KSHV-infected cells, we compared the rate of proliferation of KSHV-infected B cells in which ICN levels remained high to that of control KSHV-negative B cells with lower ICN expression levels. The results demonstrated that the rate of proliferation of the KSHV-infected BCBL1 cells was statistically higher than that of the KSHV-negative DG75 cells (Fig. 4A). Furthermore, a γ-secretase inhibitor which can block the production of ICN dramatically slowed the proliferation of BCBL1 cells, with the proliferation of DG75 cells being minimally affected by the γ-secretase inhibitor (Fig. 4A). This was most likely due to the increased levels of ICN in the infected cells. These results were further corroborated by studies examining mitotic activity by using CFSE staining (50). CFSE labels cell membranes, and the signal is proportionally lost with each generation producing new daughter cells. Cells stained with CFSE followed by treatment with the γ-secretase inhibitor for 48 h were monitored by FACS. As expected, in BCBL1 cells the mitotic activity was dramatically decreased compared to that in untreated cells (Fig. 4B, right panel). A similar effect was also observed in JSC1 cells, which are dually infected with KSHV and EBV, but with KSHV gene expression being predominant (data not shown). However, the mitotic activities of treated and untreated DG75 cells were relatively unchanged (Fig. 4B, left panel).

Previously, studies have shown that KSHV prolongs the life-span of endothelial cells (49); however, the mechanism is poorly understood. In this study, we wanted to determine if aberrant Notch signaling plays a role in this context. Thus, primary B lymphocytes were infected with the KSHV recombinant Bac36. Proliferating lymphocytes were seen by 4 weeks after infection with KSHV Bac36. However, uninfected control cells did not survive, with most cells being dead by 30 days in culture under the same conditions. FACS analysis with 7AAD staining (37) showed that only 13.3% of cells from the Bac36-infected population showed positive staining indicating death (Fig. 4C, left panel). In the uninfected population, about 41.5% of the cells were dead, with the remainder of the population being mixed with cell debris (Fig. 4C, right panel). Interestingly, when the 4-week-infected B cells were treated with γ-secretase inhibitor for 5 days, analysis by FACS showed that about 45.4% of cells had undergone death (Fig. 4D, right panel), in contrast to 21.2% of the mock-treated cells (Fig. 4D, left panel). These findings strongly suggest that KSHV prolongs the life-span of B cells, as evidenced by a >70% reduction in dead cell levels. These results indicate that ICN can contribute to the survival of KSHV-infected cells. In addition, we noticed that in the Bac36-infected group, a portion of cells were GFP positive, indicating the presence of the virus within the B cells or lymphoblastoid cells. This suggests that ICN accumulation within these cells may up-regulate cellular cytokines, supporting the growth of uninfected cells in the population through a paracrine mechanism.

Inactivation of Notch1 cleavage by γ-secretase inhibitor is responsible for G_1 arrest in KSHV-infected cells. We showed above that a γ-secretase inhibitor can dramatically slow down proliferation of the KSHV-positive BCBL1 cell line. Here we explore the potential mechanism for this decrease of the proliferating rate caused by the γ-secretase inhibitor. Cell cycle analysis of these cells showed that approximately 30% more γ-secretase inhibitor-treated BCBL1 cells than mock-treated BCBL1 cells were arrested at G_1 phase of the cell cycle (Fig. 5A). In contrast, there were no significant changes in G_1 phase of the DG75 cell cycle when these cells were treated with γ-secretase inhibitor (Fig. 5B). Moreover, Western blotting showed that ICN levels were decreased in BCBL1 cells treated with γ-secretase inhibitor (Fig. 5A). In contrast, the control DG75 cells showed similar cell cycle patterns for mock-treated cells and those treated with γ-secretase inhibitor. Additionally, Western blot analysis demonstrated that the uncleaved transmembrane form of Notch1 was the predominant signal in these cells (Fig. 5B). These results indicate that there was no active cleavage of Notch1 to the activated intracellular form in DG75 cells and explain why

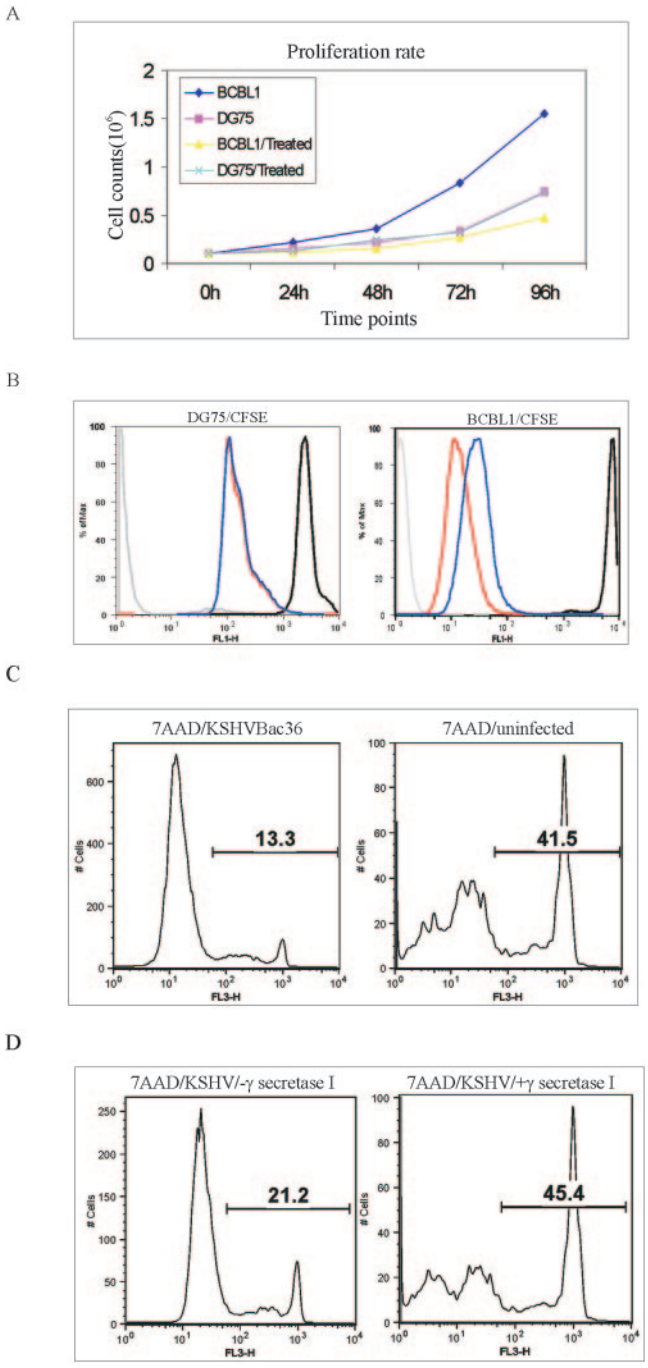

FIG. 4. (A) Comparison of proliferation rates of cells. Each cell type (100,000 cells) was cultured in RPMI 1640 with 5% BGS. At each time point, cells were stained with trypan blue and counted. The results represent three independent experiments. (B) CFSE staining showing mitosis of DG75 (left panel) and BCBL1 (right panel) cells. Five million cells were cultured in RPMI 1640 with 5% BGS and mock treated (red curves) or treated with γ-secretase inhibitor at 20 μM (blue curves). At 48 h posttreatment, cells were harvested for FACS analysis to determine mitotic activity. Gray and black curves represent negative and positive controls, respectively. The negative control was non-CFSE-staining cells, and the positive control was CFSE-staining but immediately fixed cells. (C) 7AAD staining analysis of mock-treated (left panel) and KSHV-infected (right panel) primary B cells. Two million primary B cells were mock treated or KSHV infected for 4 weeks and harvested for 7AAD staining. The percentages of dead and necrotic cells are shown. (D) Four-week KSHV-infected primary B cells were harvested and mock treated (left panel) or treated with γ-secretase inhibitor (right panel) for 5 days, and then cells were stained with 7AAD for FACS analysis.

the γ-secretase inhibitor was ineffective in regulation of cell proliferation of this KSHV-negative cell line.

Accumulation of Notch ICN up-regulates cyclin D1. Cyclin D1, a subunit of the cyclin D1/CDK2 complex, phosphorylates and inactivates the retinoblastoma protein and thus promotes progression through the G_1/S phase of the cell cycle (16, 45, 46). In the above experiments, we observed that KSHV-positive cells treated with the γ-secretase inhibitor were arrested at the G_1 phase. This indicates that elevated levels of ICN in these cells may have a role in regulation of cyclin D1. To determine if the increased levels of ICN in KSHV-infected cells led to any change in cyclin D1 levels, we screened KSHV-infected cells by Western blotting. The results demonstrated that the expression level of cyclin D1 was at least twofold higher in KSHV-infected cells than in KSHV-negative cells (Fig. 6A), with the relative density signals indicating that this could be much more and may be as high as fourfold (Fig. 6A, lower panel). Interestingly, this increase in cyclin D1 levels was a specific response to ICN levels, as cyclin D1 levels were depressed when KSHV-positive cells were treated with γ-secretase inhibitor, which blocked ICN production (Fig. 6B). Luciferase assays also indicated that the cyclin D1 promoter is responsive to ICN (Fig. 7A). Additionally, forced expression of ICN from a heterologous promoter which is not dependent on cleavage to process Notch1 to ICN in γ-secretase inhibitor-treated BCBL1 cells partially recovered the expression level of cyclin D1 (Fig. 7B). These findings strongly support the hypothesis that KSHV infection leads to an increase in ICN, stimulating proliferation of the infected cells. This effect was reversed when the cells were treated with a γ-secretase inhibitor, as shown by a reduced proliferation rate and arrest in G_1 phase.

DISCUSSION

KSHV possesses a complex series of molecular strategies to regulate cell proliferation, induce cell transformation, and prevent cell apoptosis. Indeed, a number of single gene studies have shown that different KSHV genes do possess these functional properties (12, 15, 21, 39). However, the detailed mechanism driving oncogenesis mediated by KSHV is still not clearly understood.

The initiative of this study was to explore the expression level of ICN in KSHV-positive cells because its major downstream effector, RBP-Jκ, can be targeted by KSHV LANA and Rta, two critical viral molecules involved in regulating viral latency and replication (31, 33–35). In our initial experiments, we observed that Notch ICN is aberrantly accumulated in KSHV-infected PELs. We also noticed in a recent report that ICN is up-regulated in Kaposi's sarcoma tissues (18). However, that study did not provide any potential mechanism to explain this elevated expression level of ICN in KS tissue (18). For this report, we used KSHV-infected B-lymphoma cells as a model. The cell lines used in our study were derived from PELs which

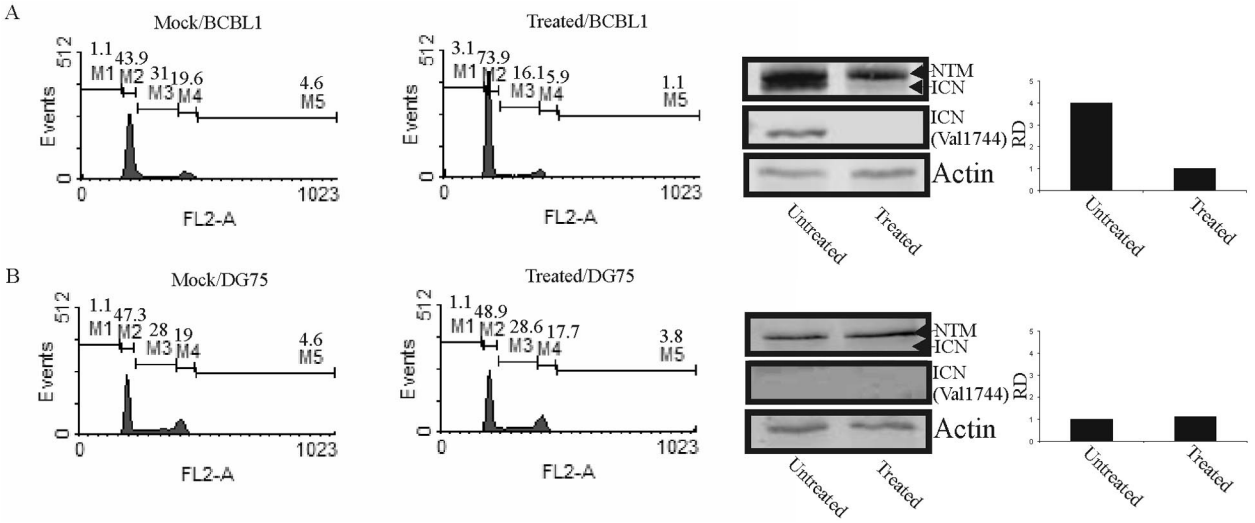

FIG. 5. FACS analysis showing cell cycle distributions of mock-treated and γ-secretase inhibitor-treated BCBL1 cells (A) and DG75 cells (B). At 48 h posttreatment, cells were harvested, fixed, and stained with propidium iodide. M2, M3, and M4 represent the G_1, S, and G_2/M populations of cells, respectively. M1 and M5 represent hypo- and hypernucleated cells, respectively. The percentage of cells in each different phase is indicated. Western blot analysis indicates the ICN levels in γ-secretase inhibitor-treated DG75 cells or BCBL1 cells. The relative density (RD) of ICN in each sample is also shown.

stably maintain the virus at 20 to 150 copies and can be cultured under standard laboratory conditions (2, 10, 13, 24, 43). This indicates that ICN accumulation is most likely due to the existence of KSHV, since ICN levels are barely detected in KSHV-negative B-lymphoma cells. More importantly, we also showed that ICN accumulation is directly related to KSHV infection by using a GFP-tagged KSHV de novo infection system. Our data further demonstrated that LANA, which is predominantly expressed in KSHV-infected B cells, can stabilize ICN, which partly explains the ICN accumulation in latently KSHV-infected cells. However, the detailed mechanism by which LANA regulates the stability of ICN is worth a more detailed exploration.

We have demonstrated that elevated ICN functionally af-

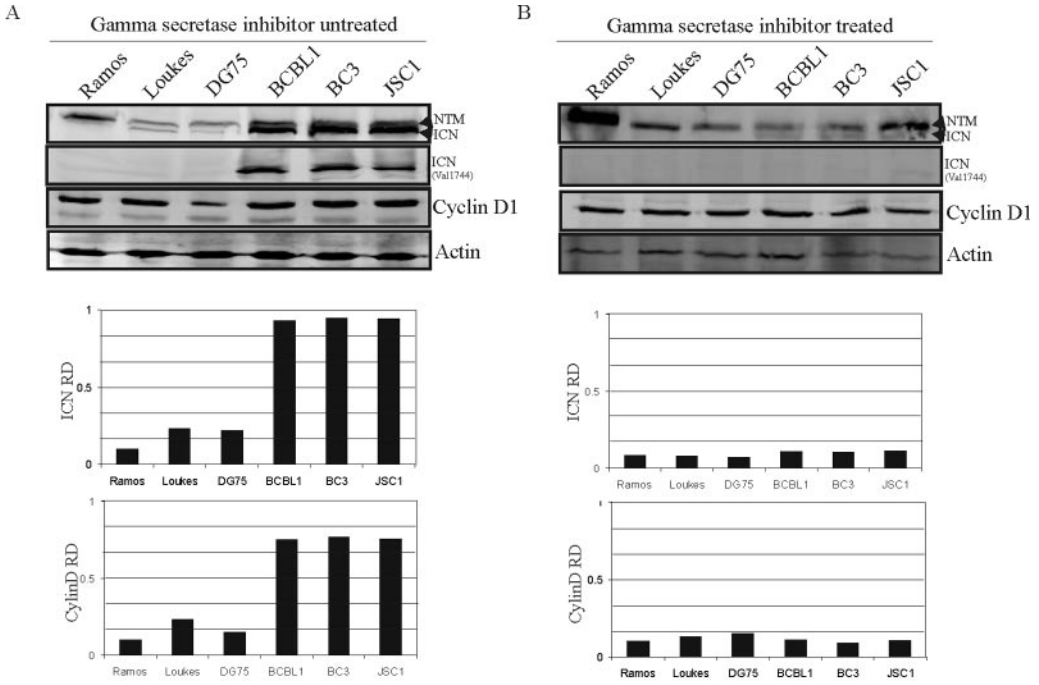

FIG. 6. (A) Western blot showing levels of NTM and ICN forms of Notch1 in different cells. The same membrane was stripped and probed for cyclin D1. (B) Western blot showing levels of NTM and ICN forms of Notch or cyclin D1 in γ-secretase inhibitor-treated cells. In both cases, the Val1744 antibody was used to confirm the presence of ICN. Quantification of the relative density (RD) of ICN or cyclin D1 is also shown.

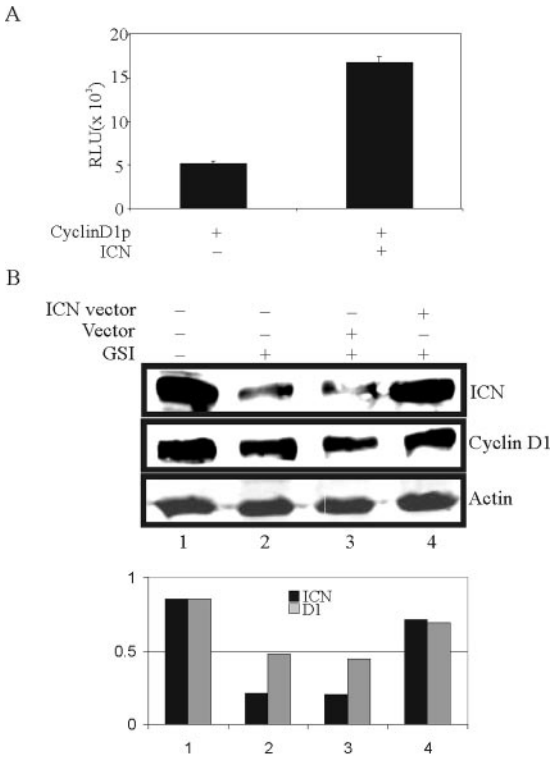

FIG. 7. (A) ICN up-regulates cyclin D1 promoter. One million U2OS cells were transfected with 0.5 μg cyclin D1 promoter reporter plasmid and 50 ng ICN expression vector or with 50 ng empty vector by the use of Lipofectamine 2000. At 24 h posttransfection, cells were harvested and lysed for a reporter assay. RLU, relative luciferase units. (B) Forced expression of ICN partially recovers the expression level of cyclin D1 in γ-secretase inhibitor (GSI)-treated BCBL1 cells. Lane 1, untreated BCBL1 cells; lane 2, BCBL1 cells with γ-secretase inhibitor; lane 3, BCBL1 cells with γ-secretase inhibitor transfected with empty vector; lane 4, BCBL1 cells with γ-secretase inhibitor transfected with pCDNA-ICN vector. The concentration of γ-secretase inhibitor was 20 μM, and the vector amount was 15 μg. The relative densities of ICN and cyclin D1 in each sample are also shown.

fects the proliferation of KSHV-positive B cells. Moreover, for the first time, we observed that ICN is critical for the survival of KSHV-infected primary B cells, since treatment with a γ-secretase inhibitor can cause cell death in KSHV-infected primary B cells. Interestingly, the γ-secretase inhibitor also resulted in apoptosis of KSHV-infected endothelial KS cells (18). The link between ICN levels and accelerated proliferation of B cells suggested a potential role for ICN in KSHV-mediated B-cell proliferation. Our data so far indicate that increased levels of expression of cyclin D1 are a direct functional consequence of ICN levels, as cyclin D1 levels were dramatically suppressed when the production of ICN was inhibited in these cells. This provides a possible explanation for the ICN-mediated increase in proliferation of KSHV-positive cells, as cyclin D1 is a major regulator of the G_1/S transition (46).

The Notch signaling pathway is highly conserved from worms to humans and plays a fundamental role in cell fate decisions, including proliferation, differentiation, and apoptosis (1). Numerous studies have also established a link between aberrant Notch signaling and oncogenesis (20, 25, 29, 40).

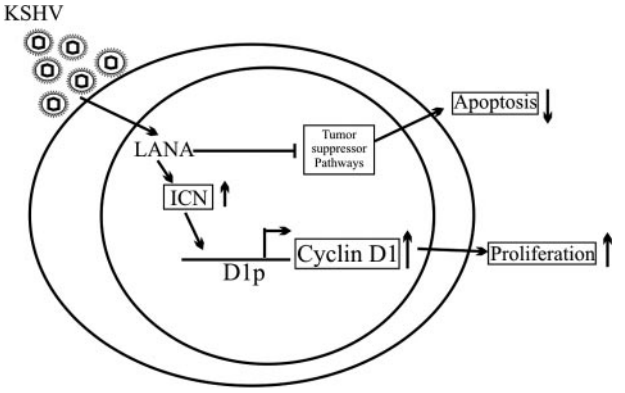

FIG. 8. Hypothetical model to show that KSHV selectively usurps the function of the Notch signaling pathway, mediating oncogenesis. In this model, LANA mediates the accumulation of Notch ICN in KSHV-positive cells through enhancement of ICN stability, either directly or indirectly. This increased level of ICN up-regulates cyclin D1, resulting in proliferation of the infected cells.

Previously, we showed that KSHV can usurp Notch signaling to modulate viral gene expression through targeting of RBP-Jκ (31). In this report, we now show that KSHV can play a direct role in terms of inducing ICN and can also usurp this signaling pathway to maintain the oncogenic phenotype of infected B-lymphoma cells.

Taken together, these results are consistent with a model in which ICN accumulates in latently KSHV-infected cells through a stabilization which is likely mediated by LANA. This increase in ICN levels is crucial for oncogenesis induced by KSHV, as seen by the significant increase in proliferation of KSHV-infected cells. The increase in proliferation mediated by ICN is also likely to be due to the up-regulation of cyclin D1 by ICN, at least in part. This provides a finely tuned model of virus-host interaction in which KSHV selectively usurps the function of a conserved cellular signaling pathway to achieve oncogenesis and provides a central role for Notch in KSHV-mediated lymphomagenesis (Fig. 8). In addition, the data showed that the γ-secretase inhibitor can dramatically reduce the proliferation of KSHV-positive cells and thus may have potential therapeutic value in the treatment of KSHV-associated human cancers.

ACKNOWLEDGMENTS

We thank Gary S. Hayward (Johns Hopkins University School of Medicine) for the KSHV Rta rabbit polyclonal antibody, Kaiji Ueda and Koichi Yamanishi (Osaka University, Osaka, Japan) for the KSHV Rta mouse monoclonal antibody, and Shoujiang Gao (University of Texas) for the Bac36 KSHV-GFP recombinant virus. We are grateful to Jie Sun (Veterinary School of the University of Pennsylvania) for technical assistance.

This work was supported by Public Health Service awards CA072510 and CA091792 from the NCI and DE01436 from NIDCR. E.S.R. is a scholar of the Leukemia and Lymphoma Society of America.

REFERENCES

1. **Artavanis-Tsakonas, S., M. D. Rand, and R. J. Lake.** 1999. Notch signaling: cell fate control and signal integration in development. Science **284:**770–776.
2. **Arvanitakis, L., E. A. Mesri, R. G. Nador, J. W. Said, A. S. Asch, D. M. Knowles, and E. Cesarman.** 1996. Establishment and characterization of a primary effusion (body cavity-based) lymphoma cell line (BC-3) harboring Kaposi's sarcoma-associated herpesvirus (KSHV/HHV-8) in the absence of Epstein-Barr virus. Blood **88:**2648–2654.

3. **Aster, J. C., E. S. Robertson, R. P. Hasserjian, J. R. Turner, E. Kieff, and J. Sklar.** 1997. Oncogenic forms of NOTCH1 lacking either the primary binding site for RBP-Jkappa or nuclear localization sequences retain the ability to associate with RBP-Jkappa and activate transcription. J. Biol. Chem. **272:**11336–11343.
4. **Ballestas, M. E., P. A. Chatis, and K. M. Kaye.** 1999. Efficient persistence of extrachromosomal KSHV DNA mediated by latency-associated nuclear antigen. Science **284:**641–644.
5. **Ballestas, M. E., and K. M. Kaye.** 2001. Kaposi's sarcoma-associated herpesvirus latency-associated nuclear antigen 1 mediates episome persistence through *cis*-acting terminal repeat (TR) sequence and specifically binds TR DNA. J. Virol. **75:**3250–3258.
6. **Berezovska, O., C. Jack, P. McLean, J. C. Aster, C. Hicks, W. Xia, M. S. Wolfe, W. T. Kimberly, G. Weinmaster, D. J. Selkoe, and B. T. Hyman.** 2000. Aspartate mutations in presenilin and gamma-secretase inhibitors both impair notch1 proteolysis and nuclear translocation with relative preservation of notch1 signaling. J. Neurochem. **75:**583–593.
7. **Bocchetta, M., L. Miele, H. I. Pass, and M. Carbone.** 2003. Notch-1 induction, a novel activity of SV40 required for growth of SV40-transformed human mesothelial cells. Oncogene **22:**81–89.
8. **Boshoff, C.** 2003. Kaposi virus scores cancer coup. Nat. Med. **9:**261–262.
9. **Boshoff, C., and R. A. Weiss.** 2001. Epidemiology and pathogenesis of Kaposi's sarcoma-associated herpesvirus. Philos. Trans. R. Soc. Lond. B **356:** 517–534.
10. **Cannon, J. S., D. Ciufo, A. L. Hawkins, C. A. Griffin, M. J. Borowitz, G. S. Hayward, and R. F. Ambinder.** 2000. A new primary effusion lymphoma-derived cell line yields a highly infectious Kaposi's sarcoma herpesvirus-containing supernatant. J. Virol. **74:**10187–10193.
11. **Cesarman, E., Y. Chang, P. S. Moore, J. W. Said, and D. M. Knowles.** 1995. Kaposi's sarcoma-associated herpesvirus-like DNA sequences in AIDS-related body-cavity-based lymphomas. N. Engl. J. Med. **332:**1186–1191.
12. **Cesarman, E., E. A. Mesri, and M. C. Gershengorn.** 2000. Viral G protein-coupled receptor and Kaposi's sarcoma: a model of paracrine neoplasia? J. Exp. Med. **191:**417–422.
13. **Cesarman, E., P. S. Moore, P. H. Rao, G. Inghirami, D. M. Knowles, and Y. Chang.** 1995. In vitro establishment and characterization of two acquired immunodeficiency syndrome-related lymphoma cell lines (BC-1 and BC-2) containing Kaposi's sarcoma-associated herpesvirus-like (KSHV) DNA sequences. Blood **86:**2708–2714.
14. **Chang, Y., E. Cesarman, M. S. Pessin, F. Lee, J. Culpepper, D. M. Knowles, and P. S. Moore.** 1994. Identification of herpesvirus-like DNA sequences in AIDS-associated Kaposi's sarcoma. Science **266:**1865–1869.
15. **Cheng, E. H., J. Nicholas, D. S. Bellows, G. S. Hayward, H. G. Guo, M. S. Reitz, and J. M. Hardwick.** 1997. A Bcl-2 homolog encoded by Kaposi sarcoma-associated virus, human herpesvirus 8, inhibits apoptosis but does not heterodimerize with Bax or Bak. Proc. Natl. Acad. Sci. USA **94:**690–694.
16. **Choudhuri, T., S. Pal, T. Das, and G. Sa.** 2005. Curcumin selectively induces apoptosis in deregulated cyclin D1-expressed cells at G_2 phase of cell cycle in a p53-dependent manner. J. Biol. Chem. **280:**20059–20068.
17. **Cotter, M. A., II, C. Subramanian, and E. S. Robertson.** 2001. The Kaposi's sarcoma-associated herpesvirus latency-associated nuclear antigen binds to specific sequences at the left end of the viral genome through its carboxy-terminus. Virology **291:**241–259.
18. **Curry, C. L., L. L. Reed, T. E. Golde, L. Miele, B. J. Nickoloff, and K. E. Foreman.** 2005. Gamma secretase inhibitor blocks Notch activation and induces apoptosis in Kaposi's sarcoma tumor cells. Oncogene **24:**6333–6344.
19. **Dourmishev, L. A., A. L. Dourmishev, D. Palmeri, R. A. Schwartz, and D. M. Lukac.** 2003. Molecular genetics of Kaposi's sarcoma-associated herpesvirus (human herpesvirus 8) epidemiology and pathogenesis. Microbiol. Mol. Biol. Rev. **67:**175–212.
20. **Ellisen, L. W., J. Bird, D. C. West, A. L. Soreng, T. C. Reynolds, S. D. Smith, and J. Sklar.** 1991. TAN-1, the human homolog of the Drosophila notch gene, is broken by chromosomal translocations in T lymphoblastic neoplasms. Cell **66:**649–661.
21. **Friborg, J., Jr., W. Kong, M. O. Hottiger, and G. J. Nabel.** 1999. p53 inhibition by the LANA protein of KSHV protects against cell death. Nature **402:**889–894.
22. **Fujimuro, M., and S. D. Hayward.** 2003. The latency-associated nuclear antigen of Kaposi's sarcoma-associated herpesvirus manipulates the activity of glycogen synthase kinase-3beta. J. Virol. **77:**8019–8030.
23. **Fujimuro, M., F. Y. Wu, C. ApRhys, H. Kajumbula, D. B. Young, G. S. Hayward, and S. D. Hayward.** 2003. A novel viral mechanism for dysregulation of beta-catenin in Kaposi's sarcoma-associated herpesvirus latency. Nat. Med. **9:**300–306.
24. **Gao, S. J., L. Kingsley, M. Li, W. Zheng, C. Parravicini, J. Ziegler, R. Newton, C. R. Rinaldo, A. Saah, J. Phair, R. Detels, Y. Chang, and P. S. Moore.** 1996. KSHV antibodies among Americans, Italians and Ugandans with and without Kaposi's sarcoma. Nat. Med. **2:**925–928.
25. **Girard, L., Z. Hanna, N. Beaulieu, C. D. Hoemann, C. Simard, C. A. Kozak, and P. Jolicoeur.** 1996. Frequent provirus insertional mutagenesis of Notch1 in thymomas of MMTVD/myc transgenic mice suggests a collaboration of c-myc and Notch1 for oncogenesis. Genes Dev. **10:**1930–1944.
26. **Greenwald, I.** 1998. LIN-12/Notch signaling: lessons from worms and flies. Genes Dev. **12:**1751–1762.
27. **Groves, A. K., M. A. Cotter, C. Subramanian, and E. S. Robertson.** 2001. The latency-associated nuclear antigen encoded by Kaposi's sarcoma-associated herpesvirus activates two major essential Epstein-Barr virus latent promoters. J. Virol. **75:**9446–9457.
28. **Hyun, T. S., C. Subramanian, M. A. Cotter II, R. A. Thomas, and E. S. Robertson.** 2001. Latency-associated nuclear antigen encoded by Kaposi's sarcoma-associated herpesvirus interacts with Tat and activates the long terminal repeat of human immunodeficiency virus type 1 in human cells. J. Virol. **75:**8761–8771.
29. **Jhappan, C., D. Gallahan, C. Stahle, E. Chu, G. H. Smith, G. Merlino, and R. Callahan.** 1992. Expression of an activated Notch-related int-3 transgene interferes with cell differentiation and induces neoplastic transformation in mammary and salivary glands. Genes Dev. **6:**345–355.
30. **Knight, J. S., M. A. Cotter II, and E. S. Robertson.** 2001. The latency-associated nuclear antigen of Kaposi's sarcoma-associated herpesvirus transactivates the telomerase reverse transcriptase promoter. J. Biol. Chem. **276:** 22971–22978.
31. **Lan, K., D. A. Kuppers, and E. S. Robertson.** 2005. Kaposi's sarcoma-associated herpesvirus reactivation is regulated by interaction of latency-associated nuclear antigen with recombination signal sequence-binding protein Jkappa, the major downstream effector of the Notch signaling pathway. J. Virol. **79:**3468–3478.
32. **Lan, K., D. A. Kuppers, S. C. Verma, and E. S. Robertson.** 2004. Kaposi's sarcoma-associated herpesvirus-encoded latency-associated nuclear antigen inhibits lytic replication by targeting Rta: a potential mechanism for virus-mediated control of latency. J. Virol. **78:**6585–6594.
33. **Lan, K., D. A. Kuppers, S. C. Verma, N. Sharma, M. Murakami, and E. S. Robertson.** 2005. Induction of Kaposi's sarcoma-associated herpesvirus latency-associated nuclear antigen by the lytic transactivator RTA: a novel mechanism for establishment of latency. J. Virol. **79:**7453–7465.
34. **Liang, Y., J. Chang, S. J. Lynch, D. M. Lukac, and D. Ganem.** 2002. The lytic switch protein of KSHV activates gene expression via functional interaction with RBP-Jkappa (CSL), the target of the Notch signaling pathway. Genes Dev. **16:**1977–1989.
35. **Liang, Y., and D. Ganem.** 2003. Lytic but not latent infection by Kaposi's sarcoma-associated herpesvirus requires host CSL protein, the mediator of Notch signaling. Proc. Natl. Acad. Sci. USA **100:**8490–8495.
36. **Ma, Q., A. J. Renzelli, K. T. Baldwin, and J. M. Antonini.** 2000. Superinduction of CYP1A1 gene expression. Regulation of 2,3,7,8-tetrachlorodibenzo-*p*-dioxin-induced degradation of Ah receptor by cycloheximide. J. Biol. Chem. **275:**12676–12683.
37. **Magner, W. J., and T. B. Tomasi.** 2005. Apoptotic and necrotic cells induced by different agents vary in their expression of MHC and costimulatory genes. Mol. Immunol. **42:**1033–1042.
38. **Moore, P. S., S. J. Gao, G. Dominguez, E. Cesarman, O. Lungu, D. M. Knowles, R. Garber, P. E. Pellett, D. J. McGeoch, and Y. Chang.** 1996. Primary characterization of a herpesvirus agent associated with Kaposi's sarcomae. J. Virol. **70:**549–558.
39. **Radkov, S. A., P. Kellam, and C. Boshoff.** 2000. The latent nuclear antigen of Kaposi sarcoma-associated herpesvirus targets the retinoblastoma-E2F pathway and with the oncogene Hras transforms primary rat cells. Nat. Med. **6:**1121–1127.
40. **Radtke, F., and K. Raj.** 2003. The role of Notch in tumorigenesis: oncogene or tumour suppressor? Nat. Rev. Cancer **3:**756–767.
41. **Renne, R., C. Barry, D. Dittmer, N. Compitello, P. O. Brown, and D. Ganem.** 2001. Modulation of cellular and viral gene expression by the latency-associated nuclear antigen of Kaposi's sarcoma-associated herpesvirus. J. Virol. **75:**458–468.
42. **Renne, R., D. Blackbourn, D. Whitby, J. Levy, and D. Ganem.** 1998. Limited transmission of Kaposi's sarcoma-associated herpesvirus in cultured cells. J. Virol. **72:**5182–5188.
43. **Renne, R., W. Zhong, B. Herndier, M. McGrath, N. Abbey, D. Kedes, and D. Ganem.** 1996. Lytic growth of Kaposi's sarcoma-associated herpesvirus (human herpesvirus 8) in culture. Nat. Med. **2:**342–346.
44. **Russo, J. J., R. A. Bohenzky, M. C. Chien, J. Chen, M. Yan, D. Maddalena, J. P. Parry, D. Peruzzi, I. S. Edelman, Y. Chang, and P. S. Moore.** 1996. Nucleotide sequence of the Kaposi sarcoma-associated herpesvirus (HHV8). Proc. Natl. Acad. Sci. USA **93:**14862–14867.
45. **Sherr, C. J., and J. M. Roberts.** 1995. Inhibitors of mammalian G_1 cyclin-dependent kinases. Genes Dev. **9:**1149–1163.
46. **Sherr, C. J., and J. M. Roberts.** 2004. Living with or without cyclins and cyclin-dependent kinases. Genes Dev. **18:**2699–2711.
47. **Si, H., and E. S. Robertson.** 2006. Kaposi's sarcoma-associated herpesvirus-encoded latency-associated nuclear antigen induces chromosomal instability through inhibition of p53 function. J. Virol. **80:**697–709.
48. **Taylor, J. L., H. N. Bennett, B. A. Snyder, P. S. Moore, and Y. Chang.** 2005. Transcriptional analysis of latent and inducible Kaposi's sarcoma-associated

herpesvirus transcripts in the K4 to K7 region. J. Virol. **79:**15099–15106.

49. **Watanabe, T., M. Sugaya, A. M. Atkins, E. A. Aquilino, A. Yang, D. L. Borris, J. Brady, and A. Blauvelt.** 2003. Kaposi's sarcoma-associated herpesvirus latency-associated nuclear antigen prolongs the life span of primary human umbilical vein endothelial cells. J. Virol. **77:**6188–6196.
50. **Wells, A. D., H. Gudmundsdottir, and L. A. Turka.** 1997. Following the fate of individual T cells throughout activation and clonal expansion. Signals from T cell receptor and CD28 differentially regulate the induction and duration of a proliferative response. J. Clin. Investig. **100:**3173–3183.
51. **Wu, L., and J. D. Griffin.** 2004. Modulation of Notch signaling by mastermind-like (MAML) transcriptional coactivators and their involvement in tumorigenesis. Semin. Cancer Biol. **14:**348–356.
52. **Zhou, F. C., Y. J. Zhang, J. H. Deng, X. P. Wang, H. Y. Pan, E. Hettler, and S. J. Gao.** 2002. Efficient infection by a recombinant Kaposi's sarcoma-associated herpesvirus cloned in a bacterial artificial chromosome: application for genetic analysis. J. Virol. **76:**6185–6196.